SOURCE AREA AND PALAEOENVIRONMENT OF THE ALBIAN UPPER BIMA SANDSTONE (B_3) YOLA ARM, NORTHERN BENUE TROUGH, NIGERIA

Supported by tetfund

Israel Abiodun Aruoriwo Etobro*, Omabehere Innocent Ejeh, and Simeon Esosa Omwanghe
Department of Geology, Delta State University, Abraka, Nigeria
*Corresponding author: aaietobro@yahoo.co.nz

Received: October 20, 2019 **Accepted:** February 11, 2020

Abstract: Field studies and laboratory analyses (granulometry and thin-section petrography of light/heavy minerals) were carried out on exposed sections of the Upper Bima Sandstone (B_3) to determine their source area(s) and depositional environment. The field studies revealed that the sediments consist of ferruginous and non-ferruginous sandstones which are made up of fine to medium-grained sandy sediments with scattered pebbles and cobbles. The B_3 is characterized by mainly planar, cross-bedded, and occasional herring-bone cross-beddings. The result of the grain-size analysis showed that the sediments are made up of medium to coarse-grained, poorly-sorted, fine-skewed and leptokurtic sandstone. The grain-shapes vary from angular to sub-angular suggesting a relatively short distance of transportation. The thin-section indicated that the sandstone averagely consists of 69.5% quartz (total quartz), 16.2% feldspar, 9.2% rock fragment and 5.1% cement. The heavy mineral separation analysis showed that the sandstone is composed of 6% rutile, 24.5% zircon, 4.3% tourmaline, 4.7% kyanite, 2.5% apatite, 1.9% sillimanite and 60.6% opaque minerals. Palaeocurrent analysis indicates the direction of ancient current to be in the SSE-NNW direction. The heavy mineral associations suggest that the ancient sediments of the B_3 in the study area were derived from nearby acidic igneous and metamorphic rocks of the Adamawa-Sardauna and Hawal Massifs belonging to the Precambrian Basement Complex of Nigeria. Fluvial to beach environment is proposed for the B_3sandstone on the basis of textural characteristics and sedimentary structures.

Keywords: Bima sandstone, grain-size analysis, palaeocurrent, palaeoenvironment, Yola arm

Introduction

The reconstruction of source area(s) for sandstones has been carried out by many analytical techniques including petrographic studies, and textural characteristics (Dickinson, 1970; Dickinson and Suczek, 1979; Zhou *et al*., 2019). The reconstruction of the source area for clastic ancient sediments involves compositional analysis to determine the origin of sediments. However, the composition of sandstones is dependent on tectonics, source lithology, climate, weathering, topography, transport, and depositional environment, thereby making their reconstruction only from petrographic analysis to be inadequate. A combination of different techniques is therefore often desirable for source area studies. Such an integrated approach always included a field study of directional sedimentary structures and light and heavy mineral analysis. Heavy mineral analysis has proven to be one of the best provenance tools because heavyminerals are thought as a resistant mineral association that survived chemical weathering during transport from their source area to the depositional site.

Palaeoenvironmental reconstruction of sandstones is another important part that determines the overall product of the sandstone after its deposition. The determination of ancient depositional environment for sandstone can be achieved by an integrated approach that involves primary sedimentary structures (e.g. cross-beddings, trace fossils,etc.), textural analysis (e.g. grain-size), geometry, and facies analysis.

Several works have been published on the Bima Sandstone Formation, Northern Benue Trough, Nigeria (Carter *et al*., 1963; Allix *et al*., 1981; Guiraud, 1990; Zaborski *et al.*, 1997; Zaborski, 2003; Samaila *et al.*, 2005; Opeloye, 2012; Tukur *et al.*, 2015). However, sediment source area(s) and palaeoenvironment of the Upper Bima (herein referred to as B_3) have not received much attention. This present study is concerned with the reconstruction of the source area and palaeoenvironment for the Albian B_3 sandstone lying between latitudes $9^0$23' to $9^0$30' N and longitudes $12^0$35' 30" to $12^0$44'E (within the Yola Arm of the Northern Benue Trough, Fig. 1) using direction sedimentary structures, textural characteristics, and light and heavy minerals petrography.

Geological setting of the Northern Benue Trough

The Benue Trough is an intra-continental sedimentary basin located in Nigeria, trending WSW-ENE (Ofoegbu, 1984). Its tectonic origin has been controversial (Olade, 1975; Benkhelil, 1989). However, it is generally thought that the trough evolved as a result of the continental separation between the South American and the African Plates during the Early Cretaceous (Guiraud *et al.*, 1992; Moulin *et al*., 2010). It is however tagged as a failed arm whose tectonic evolution is related to syn-tectonic events in a pull-apart basin (Maurin *et al.*, 1986; Benkhelil, 1989; Benkhelil *et al*., 1989; Braide 1990; 1992a). The Benue Trough is subdivided into three parts namely from south to north: Lower, Middle, and Upper; but better referred to geographically as Southern, Central, and Northern Benue Trough respectively (Nwajide, 2013).

The geology of the Northern Benue Trough has long been reported by the Geological Survey of Nigeria (Carter *et al*., 1963), describing it as separated from the Chad Basin by the Zambuk Ridge which runs roughly north-eastwards from about Gombe town through Zambuk to Biu Plateau. The Bima Sandstone has been studied by different authors including Carter *et al*. (1963), Allix *et al*. (1981), Guiraud (1990), Zaborski *et al.* (1997), Zaborski (2003), Samaila *et al.* (2005), and Tukur *et al.* (2015). This sandstone formation has a widely varied thickness ranging from 500 - 4,600 m. Allix *et al*. (1981) subdivided the Bima Sandstone into three members: the Upper (B_3), the Middle (B_2), and the Lower (B_1) (Fig. 2). Braide (1992b) and Samaila *et al*. (2005) studied the tectonic origin of pre-consolidated deformation of Bima Sandstone in the Yola Arm of Northern Benue Trough.

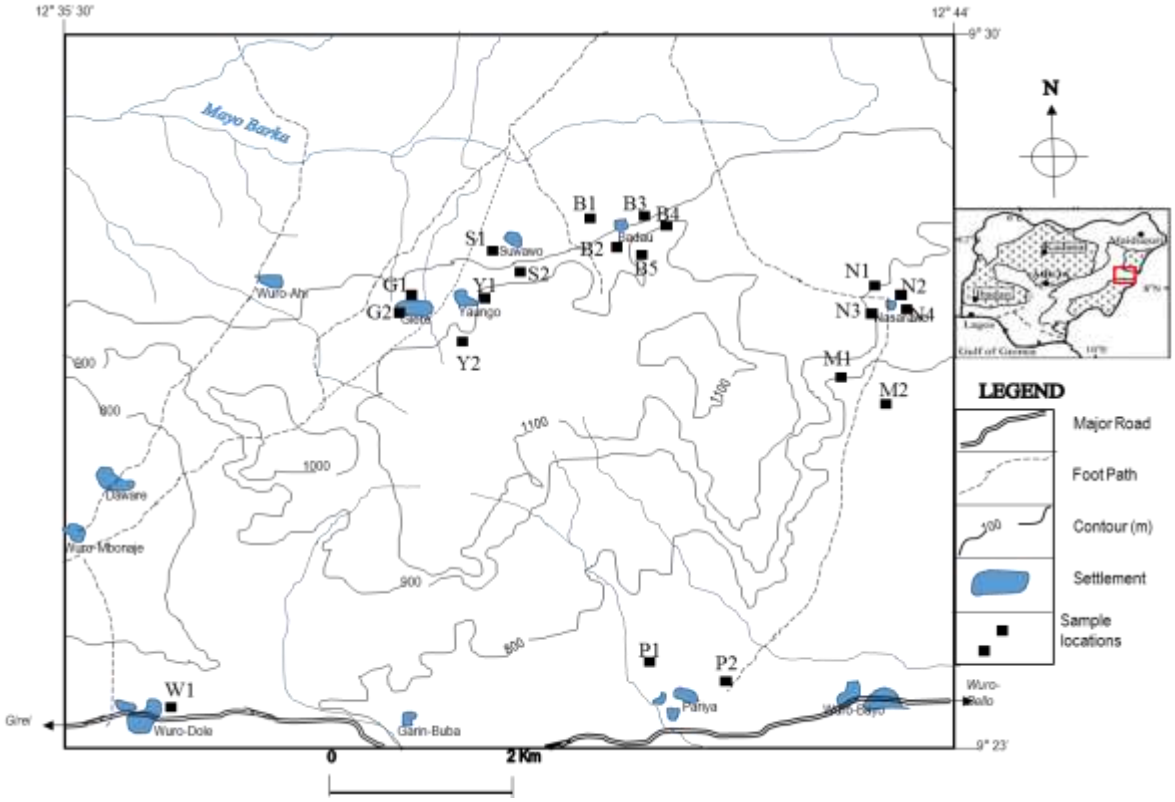

Fig. 1: Location map of the study area showing sample locations. Inset is a Geologic map of Nigeria showing the study area (red rectangle) located on the Yola Arm of the Northern Benue Trough (after Benkhelil, 1989)

AGE	PALEO-ENVIRON MENT	GONGOLA BASIN	YOLA BASIN	LAMURDE-LAU BASIN
Quaternary	Continental	Biu Basalts	Longuda Basalts	
Pliocene				
Miocene				
Oligocene		Kerri-Kerri Fm		
Eocene				
Paleocene				
Maastrichtian	Continental/ Transitional	Gombe Sandstone		
Campanian	Marine	Pindiga Formation	Lamja Sandstone	Lamja Sandstone
Santonian				
Coniacian			Numanha Fm	Numanha Fm
Turonian			Sekuleye Fm	Sekuleye Fm
Cenomanian			Jessu Fm	Jessu Fm
			Dukul Fm	Dukul Fm
		Yolde Formation		
Upper Albian	Continental	Bima Sandstone (B_3)		
Late Aptian		Bima Sandstone (B_2)		
Early Aptian		Bima Sandstone (B_1)		
Late Jurassic?				
Pre-Cambrian		Basement Complex		

Fig. 2: Stratigraphy of the Northern Benue Trough comprising of Gongola, Yola and Lamurde-Lau Basins; Where Fm= Formation (after Zaborski *et al*., 1997; Samaila *et al*., 2005)

Materials and Methods

A detailed geological mapping exercise of the B_3 sandstone was undertaken, aided by a topographical map on a scale of 1: 33,000. This involves carrying out a critical examination of the sandstone outcrops for their lithological descriptions; in-situ measurements of strike and angle of dip of directional primary structures. These strike measurements were used for an in-situ palaeocurrent analysis to infer source area(s) for the sandstone formation. Lithological sections were drawn for exposures of the formation. Representative rock samples obtainedfrom the study area and subjected to grain-size, light, and heavy minerals analyses.

Seventeen (17) sandstone samples were sieved according to the procedure of Friedman (1979). After careful disaggregation, 50 g of each sample was sieved at a mesh interval of ½ϕ. Each sample was mechanically shaken for fifteen minutes using the Ro-tap mechanical sieve shaker. By plotting cumulative frequency curves, critical percentiles (5ϕ, 16ϕ, 25ϕ, 50ϕ, 75ϕ, 84ϕ, 95ϕ) were obtained to calculate textural parameters (i.e. graphic mean size, standard deviation, inclusive graphic skewness, inclusive kurtosis, simple sorting measure, and simple skewness measure) based on the formulas proposed by Folk and Ward (1957) and Friedman (1967).

A total of sixty (60) pebbles extracted from the B_3 were subjected to pebble morphometry. This involves taking measurements of the long (L), intermediate (I) and short (S) axes of the pebbles using vernier caliper. The morphometric parameters obtained include Flatness Ratio (F.R.) and Elongation Ratio (E.R.) after Luttig (1962), Maximum Projection Sphericity Index (M.P.S.I.) after Sneed and Folk (1958) and Oblate Prolate index (O.P. index) after Dobkins and Folk (1970). The roundness of the pebbles was visually estimated following Sames (1966) chart. These parameters were evaluated as a single function and as bivariate plots of M.P.S.I. vs O.P. index (Dobkins and Folk, 1970) and Roundness vs E.R. (Sames, 1966) to discriminate depositional environments of pebbles.

Twelve (12) sandstone samples were subjected to petrographic thin-section analysis of light minerals. The sandstones were initially impregnated with resin and cut into thin sections (30 µm) before mounting on glass slides with Araldite and Canada balsam. Minerals were identified microscopically based on their optical properties under both plane-polarized light and cross-Nicols. The point-counting technique (Ingersoll *et al*., 1984) was used for the modal analysis of minerals.

The heavy mineral separation was carried-out on nine (9) sandstone samples after careful disaggregation and sieving. Bromoform with a specific gravity of 2.85 and Canada balsam was chosen as separating and mounting media respectively. Identification of heavy minerals was done under cross-Nicols and plane-polarized light on the bases of their optical characteristics.

Results and Discussion

Field studies

The geological survey revealedthat the study area is composed of sandstone occurring as high-rising ridges and occasionally low-lying. The sandstone is both massively bedded and cross-bedded (Figs. 3 and 4). It ranges from fine to coarse-grained, grading into pebbly and cobbly sandstones in some outcrop, makingsorting to be generally poor. The pebbles and cobbles sometimes tend to concentrate along the bedding planes or at the base of successive beds (Figs. 3 and 5D). The studied sandstone is generally devoid of body fossil. The lithologic sections show that the cross-bedded sandstone is composed of a successive alternation of planar cross-beddings and horizontal beddings (Fig. 3). Herring-bone cross-beddings occasionally occur in the sandstone of the study area. The sandstone formation is typically made up of fining-upward sequences (Figs. 3 and 5C). Its mineralogical composition includes quartz, feldspar, rock fragment and clay mineral. The clay mineral is whitish in colour probably suggesting kaolin that probably formed from chemical alteration of feldspathic materials. The mineralogical composition of the associated scattered pebbles in the sandstone is mainly quartz.

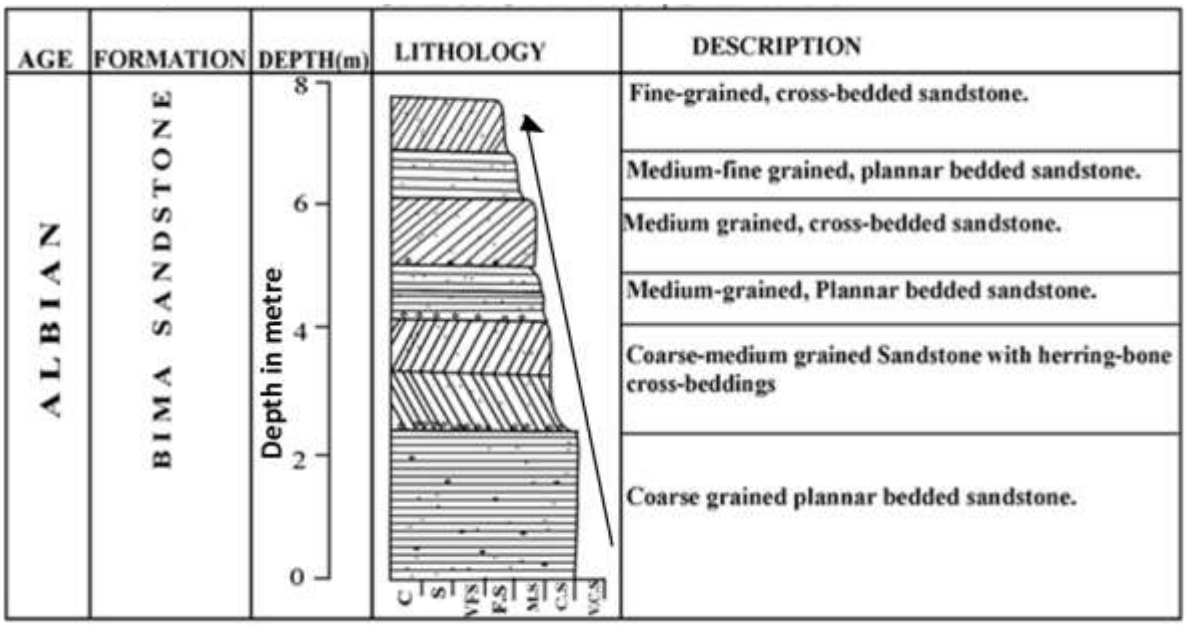

A

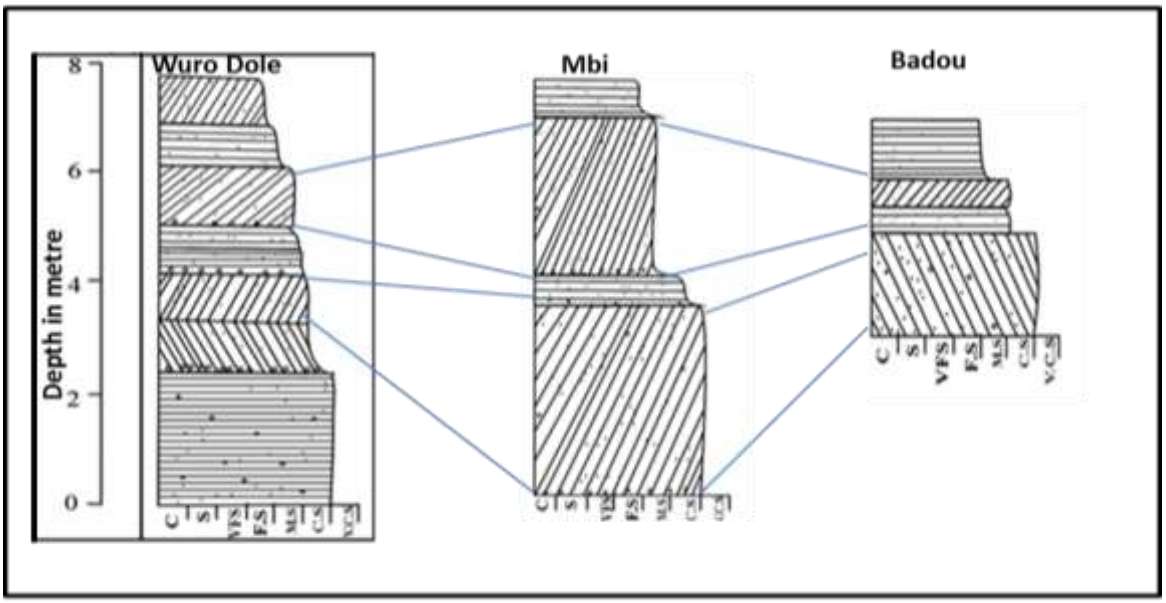

Fig. 3: Lithostratigraphy of the B_3 in the study area. A) The lithologic section displays some of the characteristic features (for example, large scale cross-bedding) of the sandstone formation. The sandstone formation is typified by fining-upward sequences. B) Correlation of lithologic sections. Note the base of the formation was not exposed in the study area. Characteristics of the formation conform to those of the B_3

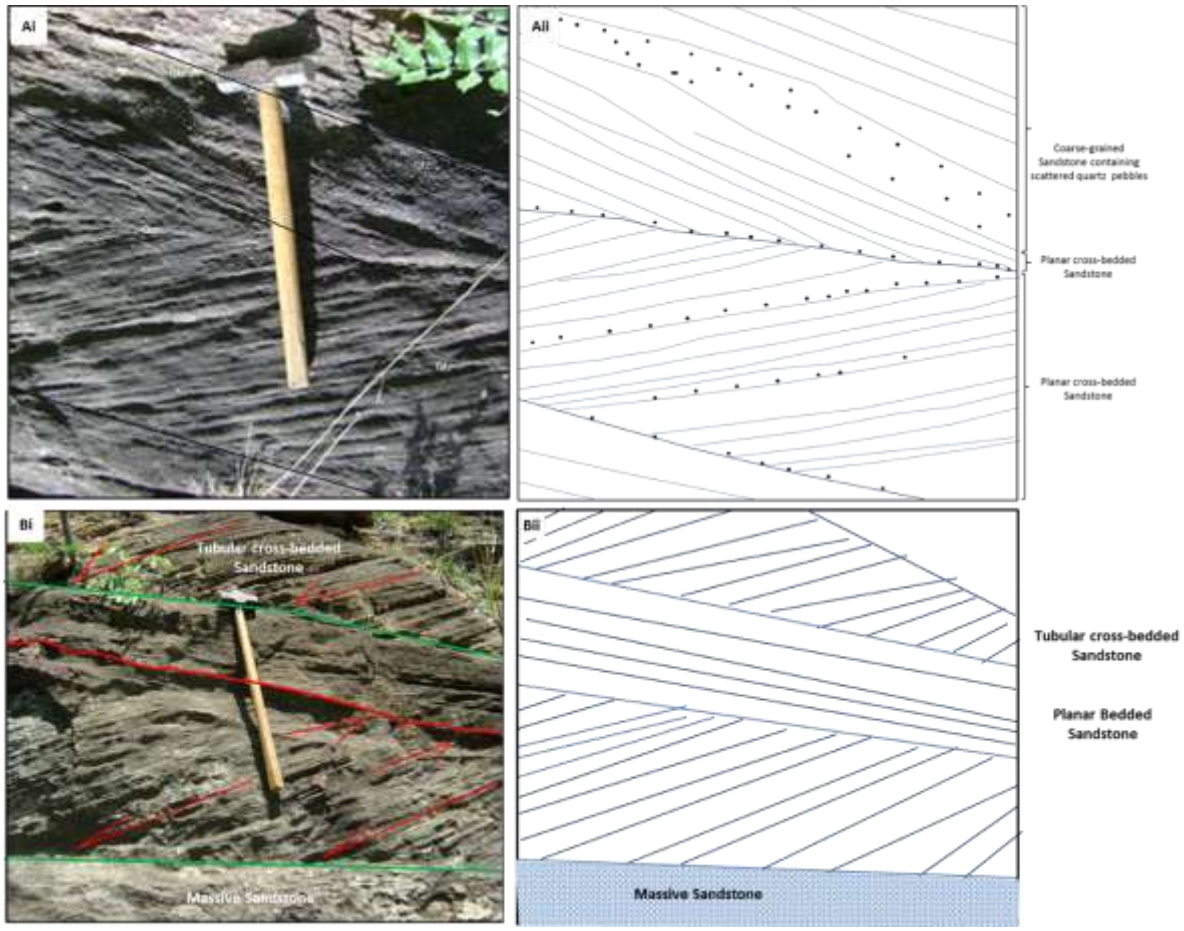

Fig. 4: Some varieties of the sandstone formation in the study area. Ai) Herring-bone cross-bedded sandstone containing some scattered pebbles within it and along its bedding planes. Bi) sequence of massive sandstone, planar cross-bedded, planar bedded sandstone and tubular cross-bedded sandstone

Fig. 5: Some different sandstone varieties of B_3 in the study area A) Fractured Thickly bedded sandstone B) Deformed tubular cross-bedded sandstone C) Planar cross-bedded sandstone underlying massive coarse-grained sandstone D) fining-upward gradation made up of a basal very coarse-grained sandstone with pebbles and cobbles and a top medium-grained sandstone

Table 1: Presentation and interpretation of the grain-size analysis of the Albian sediments of the B_3

S/N	Sample code	Graphic Mean size (ø)	Standard deviation (ø)	Graphic skewness	Graphic kurtosis	Interpretation
1	B5a	1.30	1.10	-0.01	2.32	Medium-grained, poorly-sorted, nearly symmetrical, very leptokurtic sandstone.
2	B5b	1.18	1.08	0.53	1.08	Medium-grained, poorly-sorted, strongly fine-skewed, mesokurtic sandstone
3	B5c	2.37	0.90	0.14	1.53	Fine-grained, moderately-sorted, fine-skewed, very leptokurtic sandstone
4	B5d	1.88	0.57	0.55	1.37	Medium-grained, moderately well-sorted, strongly fine skewed, leptokurtic sandstone
5	M2a	2.19	1.37	0.08	1.31	Fine-grained, poorly-sorted, nearly symmetrical, leptokurtic sandstone
6	M2b	0.73	1.46	0.25	2.29	Coarse-grained, poorly sorted, fine-skewed, very leptokurtic sandstone
7	B2a	0.42	0.91	0.16	1.37	Coarse-grained, moderately-sorted, fine-skewed, leptokurtic sandstone
8	B2b	1.77	1.32	0.03	1.33	Medium-grained, poorly-sorted, nearly symmetrical, very leptokurtic sandstone.
9	G1a	0.69	1.39	0.10	1.11	Coarse-grained, poorly-sorted, fine skewed, mesokurtic sandstone
10	G1b	0.29	1.25	0.19	1.29	Coarse-grained, poorly-sorted, fine skewed, leptokurtic sandstone
11	N2a	1.77	1.17	0.56	1.50	Medium-grained, poorly sorted, strongly fine skewed, leptokurtic sandstone
12	N2b	1.42	1.16	0.37	1.57	Medium-grained, poorly-sorted, strongly fine skewed, very leptokurtic sandstone
13	B5e	1.96	0.89	-0.06	1.39	Medium-grained, moderately-sorted, nearly symmetrical, leptokurtic sandstone.
14	W1	1.34	0.88	-0.34	1.18	Medium-grained, moderately-sorted, strongly coarse-skewed, leptokurtic sandstone.
15	Y2	-0.33	2.26	0.10	0.07	Very coarse-grained, poorly-sorted fine skewed, very platykurtic sandstone,
16	N1	2.76	0.80	0.02	2.19	Fine-grained, moderately-sorted, nearly symmetrical, very leptokurtic sandstone
17	S2	2.99	0.89	0.30	1.38	Fine-grained, moderately-sorted, fine skewed, leptokurtic sandstone
Average		**1.45**	**1.14**	**0.17**	**1.43**	Medium-grained, poorly-sorted, fine-skewed, leptokurtic sandstone

Grain-size and textural studies

Both sieving and pebble morphometric methods were used to determine the size distribution of the particles of ancient sediments of the B_3.

Sieving

The graphic mean size of the sediments that make up the B_3sandstone in the study area ranges from -0.33 (very coarse-grained) to 2.99ϕ (fine-grained) (averagely 1.45ϕ, medium-grained) (Wentworth, 1922) (Table 1). The standard deviation which is a measure of sorting ranges from 0.57 to 2.26ϕ (averagely 1.14ϕ); these imply that the sandstone is moderately well-sorted to very poorly-sorted (averagely poorly-sorted) (Folk and Ward, 1957). Inclusive skewness values vary from -0.13 to 0.56 (averagely 0.19) indicating coarse-skewed to strongly fine-skewed (averagely fine-skewed). Graphic kurtosis ranges from 0.07 to 2.32 (1.43 on the average) (Table 1), suggesting very platykurtic to very leptokurtic (averagely leptokurtic) sandstone.

Pebble morphometry

Many authors have established the usefulness of pebble morphometry in palaeoenvironmental reconstructions (e.g. Luttig, 1962; Sames, 1966; Dobkin and Folk, 1970; Nwajide and Hoque, 1982). For examples, E.R., M.P.S.I., O.P. index, form, and roundness have been employed as indices for the inferences of depositional environments for ancient sediments. The O.P. index values (Table 2) range from -6.93 to 10.9 (average 2.85) with over 85% of these values greater than -1.5 which is the lower limit value of O.P index for pebbles deposited in fluvial environment (e.g. Dobkins and Folk, 1970). This, therefore, implies that the Albian sediments of the B3 were probably deposited in a fluvial environment. The average M.P.S.I. value for the pebbles associated with the Albian sediments of the B3 is 0.72, implying deposition in a fluvial setting since it is above the threshold value (0.65) for sedimentation in a fluvial environment (Dobkin and Folk, 1970). Pebble roundness is a weak palaeoenvironmental indicator, because it is a function of transport distance. Pebble roundness, however, increases from river to beach (Sneed and Folk, 1958). The average pebble roundness of the studied pebbles is 43% suggesting a deposition under fluvial environment since it is below 46% set as the upper limit for fluvial pebbles (Sames, 1966). Environmental discrimination using scatter plots of maximum projection sphericity index (M.P.S.I.) versus oblate prolate (O.P) index (Fig. 6A) and roundness versus elongation ratio (E.R.; Fig. 6B) was applied for the B_3 sandstone. The bivariate plot of M.P.S.I against O.P. index indicates that about 90% of the ancient sediments accumulated under fluvial conditions while 10% deposited in a beach environment (Fig. 6A). The scatter plot of roundness versus E.R. suggests that about 60% of the sediments deposited in a fluvial setting and the remaining 40% under littoral conditions (Fig. 6B).

Table 2: Pebble form indices for pebbles from the B_3

S/N	L (cm)	I (cm)	S (cm)	F.R. (S/L)	E.R. (I/L)	MPSI	O.P. Index	R'dness (%)
1	4.75	2.07	1.85	0.39	0.44	0.70	10.90	10
2	4.82	2.89	2.71	0.56	0.60	0.81	7.38	40
3	4.15	2.79	2.45	0.59	0.67	0.80	5.085	40
4	4.92	3.38	2.96	0.60	0.69	0.81	4.75	50
5	3.23	2.92	1.79	0.55	0.90	0.70	-5.14	25
6	3.69	2.22	2.15	0.58	0.58	0.83	7.80	40
7	4.28	3.37	2.84	0.66	0.79	0.82	1.99	10
8	2.64	2.08	1.55	0.59	0.79	0.76	0.23	60
9	2.72	2.11	1.55	0.57	0.78	0.75	0.38	30
10	3.33	2.12	2.09	0.63	0.64	0.85	7.58	40
11	3.79	2.35	1.90	0.50	0.62	0.74	5.23	30
12	4.68	2.19	1.96	0.42	0.47	0.72	9.92	50
13	3.99	3.45	2.20	0.55	0.87	0.71	-3.60	25
14	3.01	2.02	1.53	0.51	0.67	0.73	3.33	40
15	4.02	2.96	1.64	0.41	0.74	0.61	-1.34	40
16	3.16	2.75	1.72	0.54	0.87	0.70	-3.96	25
17	3.29	2.66	2.20	0.67	0.81	0.82	1.17	50
18	3.88	2.17	1.95	0.50	0.56	0.77	7.67	30
19	3.67	2.15	1.72	0.47	0.59	0.72	5.96	20
20	4.69	2.49	1.75	0.37	0.53	0.64	6.66	30
21	4.18	2.70	1.60	0.38	0.65	0.61	1.92	10
22	3.02	1.80	1.75	0.58	0.60	0.82	7.96	30
23	5.06	2.60	2.23	0.44	0.52	0.73	0.83	40
24	3.40	2.92	1.50	0.44	0.86	0.61	-5.61	20
25	3.90	3.10	2.19	0.56	0.80	0.74	-0.57	25
26	4.06	2.06	2.01	0.50	0.51	0.79	9.61	20
27	2.86	2.03	1.50	0.53	0.71	0.73	2.10	30
28	4.37	1.96	1.85	0.42	0.45	0.74	10.79	40
29	3.18	2.00	1.67	0.53	0.63	0.76	5.36	25
30	2.90	2.40	1.70	0.59	0.83	0.75	-1.42	60
31	2.84	2.20	1.47	0.52	0.78	0.70	-0.63	25
32	2.98	2.20	1.50	0.50	0.74	0.70	0.53	60
33	2.56	2.00	2.00	0.80	0.80	0.93	6.25	50
34	3.45	2.00	1.45	0.42	0.58	0.67	5.36	20
35	3.62	2.71	2.12	0.42	0.57	0.63	5.36	20
36	4.35	2.50	1.57	0.36	0.57	0.61	4.58	30
37	4.99	2.60	2.30	0.46	0.52	0.74	8.43	30
38	3.10	2.34	2.16	0.70	0.76	0.86	0.43	50
39	2.83	2.19	1.90	0.80	0.92	0.89	-1.31	50
40	2.83	2.10	1.84	0.65	0.74	0.83	3.62	30
41	2.40	2.30	1.50	0.63	0.96	0.74	-6.93	60
42	2.96	2.00	1.50	0.53	0.68	0.75	3.40	20
43	2.76	1.62	0.95	0.34	0.59	0.59	3.77	40
44	2.50	2.44	2.44	0.98	0.98	0.99	5.12	80
45	6.00	3.99	2.67	0.45	0.67	0.67	2.33	90
46	3.16	2.42	1.78	0.56	0.77	0.75	0.64	90
47	2.70	2.35	1.80	0.67	0.87	0.80	-1.67	60
48	3.80	2.82	2.48	0.66	0.74	0.83	3.70	90
49	3.32	2.22	2.05	0.62	0.67	0.83	5.93	50
50	2.35	2.20	2.20	0.94	0.94	0.98	5.34	80
51	2.23	1.65	1.35	0.61	0.74	0.79	2.63	90
52	2.46	2.13	1.80	0.73	0.87	0.85	0.00	60
53	3.35	2.71	2.36	0.71	0.81	0.85	2.08	50
54	3.24	2.48	2.12	0.65	0.76	0.82	2.73	50
55	3.62	3.20	2.70	0.75	0.88	0.86	-0.58	50
56	4.34	2.85	2.10	0.48	0.66	0.71	3.41	40
57	2.25	2.22	2.08	0.92	0.99	0.95	-3.50	80
58	2.84	2.00	1.82	0.64	0.70	0.84	5.05	60
59	3.20	2.10	1.50	0.47	0.66	0.69	3.14	50
60	2.69	2.49	1.64	0.61	0.93	0.74	-5.07	40
Average	**3.48**	**2.43**	**1.93**	**0.57**	**0.72**	**0.77**	**2.85**	**43**

Where L, I, and S are Long, Intermediate, Short axes respectively; while O.P., M.P.S.I., F. R., and E.R. are as stated in the text; R'dness = Roundness

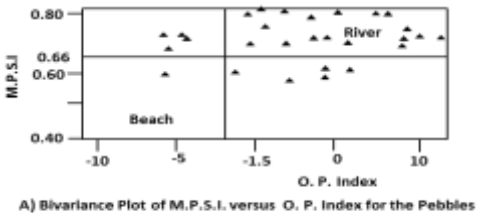

A) Bivariance Plot of M.P.S.I. versus O. P. Index for the Pebbles

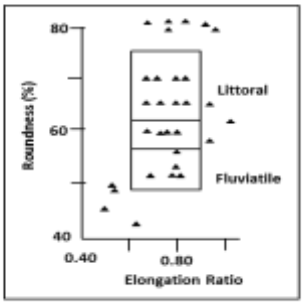

B) Bivariance Plot of Pebble Roundness against Elongation Ratio

Fig. 6: Bivariate plots based on pebble morphometric analysis. A) The plot ofM.P.S.I. versus O.P. index. B) Pebble roundness against E.R. obtained for the B_3

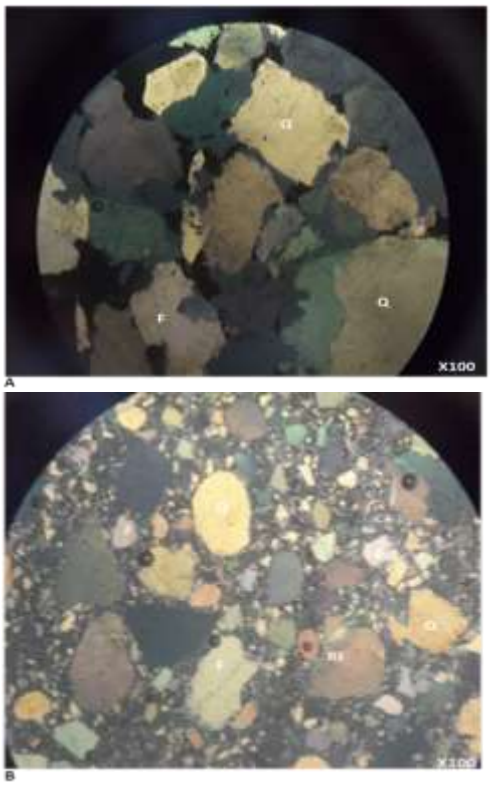

Fig. 7: Photomicrographs of mineralogical composition of the B_3. A) Very coarse-grained sandstone. B). Poorly-sorted sandstone; Where Q= quartz; F= feldspar; RF= rock fragments

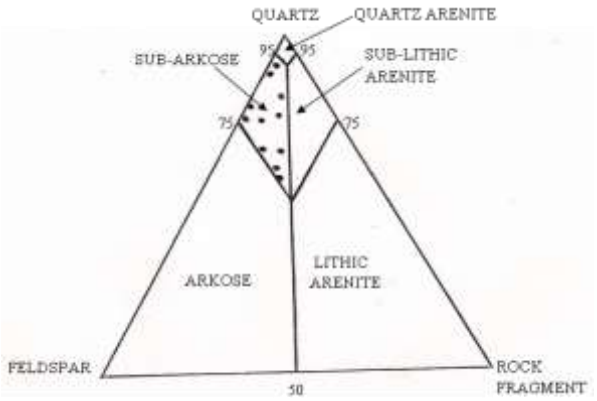

Fig. 8: Ternary diagram plotted for the B_3 on the basis of the framework composition of quartz, feldspar and rock fragments

Petrographic study

Light mineral petrography

Petrographic study of the B_3sandstone shows that it consists of about 69.5% quartz, 16.2% feldspar, 9.2% rock fragment and 5.1% haematite (Table 3) acting as the cementing material. It further indicates that the grains range generally from angular to sub-angular in shape and they are loose- to closely-packed (Figs. 7A and B). Following the sandstone classification of Pettijohn *et al*. (1973) based on the framework composition of quartz, feldspar, and rock fragmenton a ternary diagram, the B_3sandstone is grouped as mainly sub-arkose (Fig. 8).

Table 3: Petrographic properties of the detrital components of the B_3

Sample Code.	Grain Size	Sorting	Grain Shape	Quartz (%)	Feldspar (%)	Rock Fragment (%)	Cement (%)
M1	Coarse-grained	Poorly-sorted	Angular	83.3	11.1	-	5.5
B3b	Medium-grained	Moderately well-sorted	Angular	68.4	21	-	10.5
B2b	Medium-grained	Poorly-sorted	Angular	68.8	18.75	6.3	6.3
P1	Medium-grained	Well-sorted	Sub-angular	77.4	19.4	-	3.2
M2b	Coarse-grained	Well-sorted	Sub-angular	57.1	14.3	14.3	14.1
B1	Coarse-grained	Poorly sorted	Sub-angular	66.7	23.8	9.5	-
B2a	Coarse-grained	Well-sorted	Sub-angular	58.5	7.1	-	7.1
B4b	Medium-grained	Well-sorted	Sub-angular	61.5	23.1	15.4	-
B4a	Medium-grained	Well-sorted	Sub-angular	61.5	23.1	15.4	-
W1	Very coarse-grained	Poorly-sorted	Angular	55.6	22.2	16.1	5.6
N2a	Medium-grained	Poorly-sorted	Sub-angular	76.9	11.5	7.7	3.9
M2a	Medium-grained	Poorly-sorted	Angular	71.4	14.3	9.7	4.8

Table 4: Modal composition of the heavy mineral separation analysis result of B_3 in the study area

Sample code	Opaque Minerals (%)	Non – Opaque Minerals (%)						ZTR index (%)	Maturity status
		Rutile	Zircon	Tourmaline	Kyanite	Apatite	Silimanite		
B5b	49.0	06.0	24.5	11.8	-	03.9	03.9	84.4	Matured
G1b	55.6	11.1	22.2	-	11.1	-	-	75.0	Matured
Y2	66.7	19.1	-	-	14.3	-	04.8	50.0	Immature to sub-matured
N1	59.6	07.7	17.3	5.8	03.8	01.9	03.8	76.6	Matured
S2	25.0	02.1	54.2	10.4	-	08.3	-	89.5	Matured
B5b	46.9	08.2	30.6	06.1	-	06.1	02.0	84.7	Matured
G1a	83.3	-	10.0	04.2	04.2	-	-	77.2	Matured
M2a	85.0	-	07.5	-	05.0	02.5	-	50.0	Immature to sub-matured
M2b	73.7	-	21.1	-	00.6	-	02.6	80.2	Matured
Average	**60.6**	**06.0**	**20.8**	**04.3**	**04.7**	**02.5**	**01.9**	**77.5**	**Matured**

Heavy-mineral petrography

Heavy minerals are useful tools for provenance studies as they give insight into the nature of the parent rock(s) due to their high resistance to weathering and the ability to survive chemical alteration. They are also diagnostic features of certain kind of parent rocks (e.g. Friedman and Sanders, 1978). The heavy mineral separation analysis reveals that the ancient sediments consist of both opaque and non-opaque heavy minerals. The microscopic study shows that the non-opaque heavy minerals (Table 4) include rutile (6%), zircon (20.8%), tourmaline (4.3%), kyanite (4.7%), apatite (2.5%) and sillimanite (1.9%). ZTR index (i.e. percentage of ultrastable- zircon, rutile and tourmaline in the total non-opaque heavy mineral fractions) often gives a measure of the degree of dissolution which took place in clastic sedimentary rock (Hubert, 1962). The computed ZTR indices for the analysed samples show a range from 50.0 to 89.5% (average 77.5%). Only two of the analysed samples have ZTR indices less than 75% (i.e. the lower limit of mineralogical maturity; Hubbert, 1962) suggesting that nearly all the ancient sediments of the B_3 are mineralogically matured (Table 4).

Source area

The main purpose of provenance studies is the characterisation of the source area(s) through assessment/measurements of compositional materials and textural properties of sediments, augmented by data from other relevant sources (Pettijohn *et al.*, 1987; Weltje and von Eynatten, 2004). However, directional sedimentary structuresand light/heavy minerals, and grain-shapewere utilized in this work to determine the source area of the sediment in the study area.

Evidence from directional sedimentary structures and texture

The angular to sub-angular (Figs. 7A and B) grains of the sandstones suggest that the ancient sediments were derived from nearby source rocks, from which detritus were transported for a short distance (Friedman and Sanders, 1978). The azimuth directions of the cross-beddings associated with the B_3 sandstone in the study area plotted on a rose-current diagram (with a class interval of 10°) indicates a bimodal direction comprising mostly SSE-NNW, and to a lesser degree NE-SW direction (Fig. 9); suggesting that the ancient sediments were mainly derived from the SSE and NE directions corresponding Precambrian Basement Complex rocks of Adamawa Sardauna and Hawal Massifs respectively (Fig. 10). They include granites and gneisses. The ancient sandy sediments of the B_3 probably were deposited during the Late Albian to Cenomanian regressive phase that generally affected the Benue Trough (Whiteman, 1982).

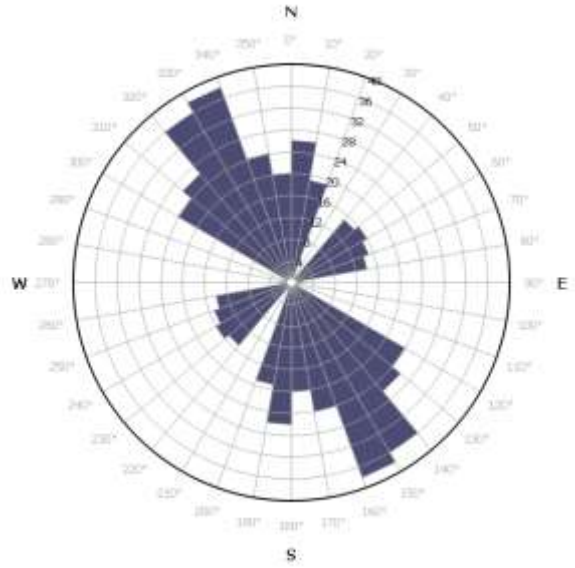

Fig. 9: A composite rose-current diagram obtained for the B_3 in the study area

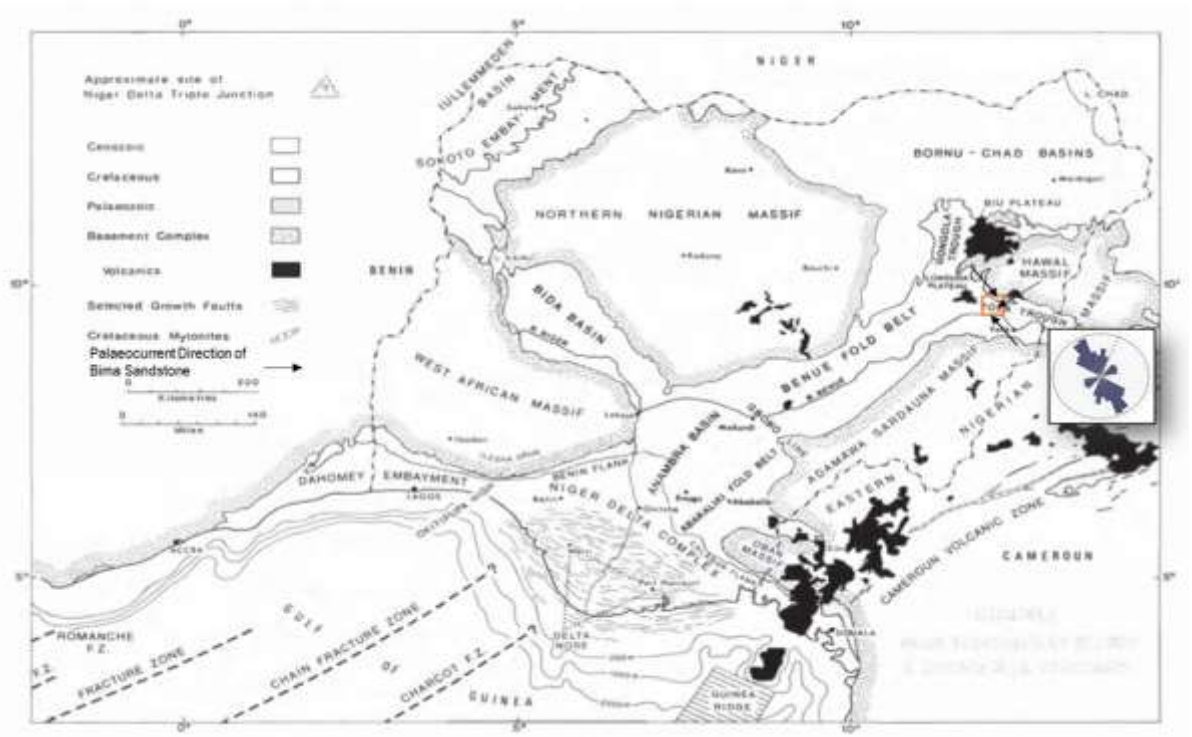

Fig. 10: Geologic map of Nigeria (modified after Whiteman, 1982); Inset is a rose current diagram plotted fof study area marked with a rectangle

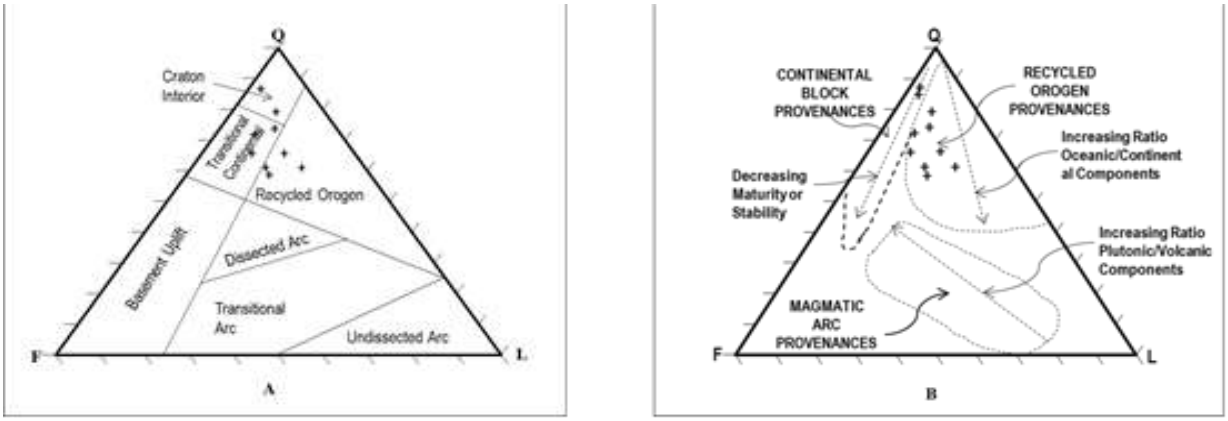

Fig. 11: Ternary diagrams based on modal framework composition of quartz (Q), feldspar (F), and rock fragment (L) plotted for the ancient sediments of the B_3 to infer its source areas based on A) Dickinson et al. (1983) and, B) Dickinson and Suczek (1979)

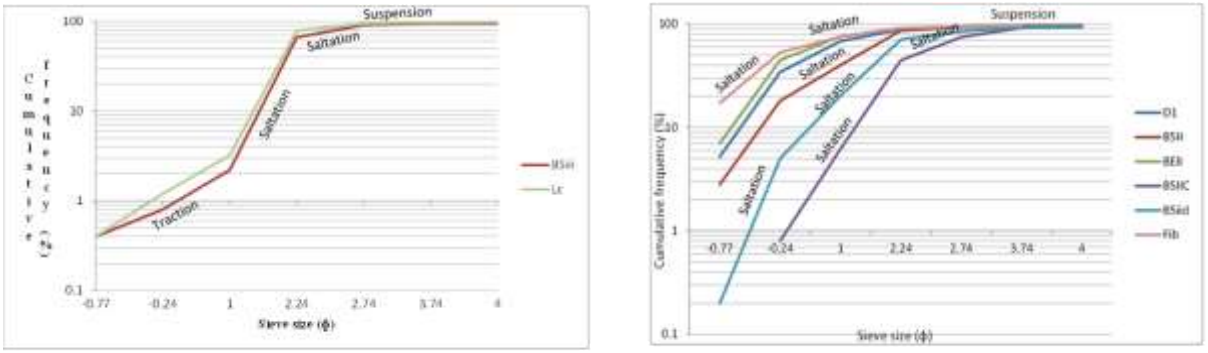

Fig. 12: Cumulative frequency plots on semi-log probability paper showing: A) 3- segment populations (one suspension, and two saltation populations), and B) 4-segment populations (one suspension, two saltation and one traction populations) for the B_3 of the study area.

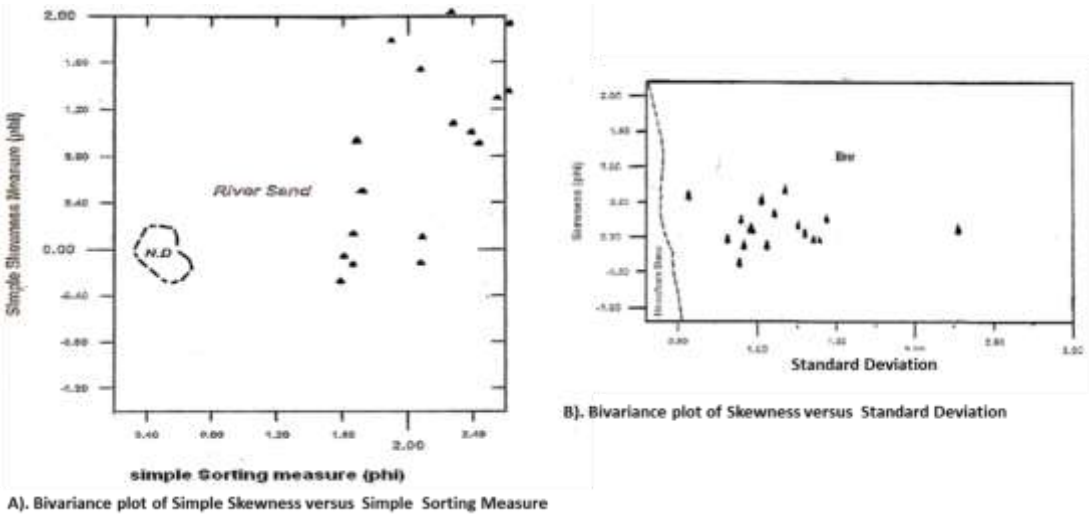

Fig. 13: Environmental discrimination plots using statistical parameters obtained from the grain-size analysis for the B_3: A) Bivariate plots of simple skewness versus simple sorting measure; B) skewness against standard deviation

Evidence from light and heavy minerals

Following Dickinson *et al*. (1983) and Dickinson and Suczek (1979), the quartz (Q), feldspar (F), and rock fragments (L) were plotted on QFL ternary diagrams (Figs. 11A and B) to infer source area(s) for the B_3 sandstone. Both QFL ternary diagrams depict that most of the ancient sandy sediments were sourced from recycled orogen, while few were from continental source areas (Figs. 11A and B). The QFL ternary diagram of Dickinson *et al*. (1983) however suggests that some of the ancient sandy sediments were products of craton interior (Fig. 11A). The mineralogically sub-mature to immature ancient sediments of the B_3 sandstone formation also indicate that they were derived from the breakdown of basement rocks and selective preservation of >10 % feldspar during short distance/short duration transport and deposition. The occurrence of rutile, zircon, apatite, and tourmaline in the

heavy mineral suite indicates acidic igneous rocks; while sillimanite and kyanite are indicative of high-grade metamorphic source (Tickell, 1931; Hubert, 1962; Friedman and Sanders, 1978; Boggs, 2009).

Palaeoenvironment

Evidence from field studies

Sedimentary structures are useful features for environmental reconstruction because they clearly reveal the depositional processes which laid down the sediments (Selley, 1975). Sedimentary structures encountered in the study area are mainly cross-beddings and laminations. The presence of primary structures such as planar cross-beddings and laminations in the B_3sandstone in the study area, coupled with the fining upward succession in grain sizes, and the absence of body fossils generally suggests a fluvial environment of deposition. The association of the herring-bone cross-beddings, however, suggests deposition in a beach (littoral) to the tidal environment since the herring-bone cross-beddings often depict sediment transport in two opposing directions by tidal currents (e.g. Friedman and Sanders, 1978).

Evidence from textural characteristics

The parameters used in deducing the ancient environment of deposition in this study are textural characteristics and sedimentary structures of the sandstone formation. The pebbly sandstones are typically high energy deposits under turbulent environment.Attempts have been made by various workers such as Martins (1965); Visher (1969); Friedman and Sanders (1978); Pettijohn (1984); Tucker (1988); Martins *et al*. (1997); and Martins (2003) to relate statistical parameters of grain-size distribution to environmental diagnosis. According to Awasthi (1970), among the grain-size parameters of clastic sediments, a sign of skewness is the most sensitive to environmental conditions. About 83% of the analysed sandstones are positively skewed while only 17% are negatively skewed. Sediments that are skewed positively often point to a calm and steady energy environment while negatively skewed sediments are suggestive of turbulent energy (Awasthi, 1970). The cumulative frequency curves plotted on probability paper indicated mainly three segments (Fig. 12A) while a few of them are made up of four segments (Fig. 12B). The three segments comprise two saltation populations and one suspension population while the four segments consist of one traction population, two saltation populations, and one suspension population (Figs. 12A and B).

The generalabsence of traction population (Fig. 12A) for most of the samples analyzed suggests a fluvial setting (Visher, 1969). Thus, most of the ancient sediments of the B_3 were transported by both saltation and suspension processes. These suggest that low to moderate energy prevailed during their transportation.Following Friedman and Sanders, (1978), such suspension-saltation population is typical of most river environments. However, the four-segment populations (Fig. 12B) depict deposition in a beach environment.Both scatter plots of simple skewness measure versus simple sorting measure (Fig. 13A) and skewness against standard deviation (Fig. 13B) obtained for the ancient sediments of the B_3sandstone suggest that most of the ancient sediments were deposited mainly under fluvial condition (Friedman, 1975).

Conclusion

This study has shown that B_3 sandstone is averagely medium-grained, poorly-sorted, fine-skewed and leptokurtic sandstone. It ranges in shape from angular to sub-angular, which suggest that the sediments travelled a relatively short distance from their parent rocks to where they were finally deposited.

The petrographic study of thin-section slides revealed the presence of quartz, feldspar, rock fragment and haematite acting as the cementing material. The sandstone is mainly sub-arkose as indicated on the ternary diagram of quartz, feldspar and rock fragment. The heavy mineral suite includes rutile, zircon, tourmaline, kyanite, apatite, sillimanite, and opaque minerals. The occurrences of these minerals indicate igneous and metamorphic rocks as the parent rocks. The high proportion of quartz to feldspar, as well as the occurrences of zircon, tourmaline and rutile, and a high value of maturity index make the sandstone mineralogically matured. The result obtained from paleocurrent analysis showed that the ancient current direction is in the SSE-NNW direction which means that the source area(s) of the sediments are in the SSE region. There is however another minor source area in the NE direction. The result from cumulative frequency curves plotted on probability paper, scatter plots of simple skewness measure versus simple sorting measure, skewness versus standard deviation, M.PS.I versus O.P index and roundness versus E.R. of the pebbles of the B_3in the study area indicate fluvial environment. The herring-bone cross-bedding, however, suggests a beach environment.

Generally, the results and inferences obtained from this study show the Albian sediments of the B_3 in the study area were sourced from acidic igneous and metamorphic rocks of the Adamawa-Sardauna and Hawal Massifs of the Nigerian Basement Complex. These ancient sediments accumulated in a range of environments from mainly fluvial to beach environments.

Conflict of Interest

Authors declare that there is no conflict of interest related to this study.

References

Allix P, Grosdidier E, Jardine S, Legoux O & Popoff M 1981. Découverte d' Aptien Superieur à Albien inférieur daté par microfossiles dans la serie detritique Cretacée du fossé de la Bénoué (Nigeria). C.R. Acad. Sci., Pari, pp. 292, 1291-1294.

Awasthi AK 1970. Skewness as an environmental indicator in the Solani river system, Roorkee (India). *Sed. Geol*., 4(1-2): 177-183.

Benkhelil MJ 1989. The origin and evolution of the Cretaceous Benue Trough, Nigeria. *J. Afri. Earth Sci*., 8: 251-282.

Benkhelil MJ, Guiraud M, Ponsard JF & Saugy L 1989. The Bornu-Benue Trough, the Niger Delta and its Offshore: Tectono-sedimentary reconstruction during the Cretaceous and Tertiary from geophysical data and geology. In: Kogbe, C. A. (Ed): Geology of Nigeria. Rockview (Nigeria) Limited, Jos; 277-309.

Boggs S 2009. Petrology of sedimentary rocks. 2nd Edition. Cambridge University Press, Cambridge p. 612.

Braide SP 1990. Studies on the sedimentology and tectonics of the Yola Arm of the Benue Trough: Facies architecture and their tectonic significance. *J. Min. and Geol*., 28: 23-31.

Braide, S.P., 1992a. Tectonic origin of pre-consolidation deformation Bima Sandstone. *Nig. Ass. Petrol. Geol. Bull*., 7(1): 39–45.

Braide SP 1992b. Morphology and depositional history of an Aptian–Albian crevasse splay in the Albian Bima Sandstone, Yola Basin, Benue Trough. *Nig. Ass. Petrol. Geol. Bull*., 7(1): 39–45.

Carter JD, Barber W, Tait EA & Jones JP 1963. The geology of parts of Adamawa, Bauchi and Bornu provinces in northeastern Nigeria. *Bull. Geol. Sur. Nig*., 30: 109.

Dickinson WR 1970. Interpreting detrital modes of greywacke and arkose. *J. Sed. Petrol.*, 40(2): 695-707.

Dickinson WR & Suczek C 1979. Plate tectonics and sandstone composition. *Ame. Ass. Pet. Geol. Bull*., 63, :164–2192.

Dickinson WR, Beard S, Brakenbridge F, Erjavec J, Ferguson R, Inman K, Knepp R, Lindberg P & Ryberg P 1983. Provenance of North American Phanerozoic sandstones in relation to tectonic setting. *Geol. Soc. Ame. Bull*., 64: 233–235.

Dobkins JE & Folk RL 1970. Shape development on Tahiti-Nui. *J. Sed. Petrol*., 40: 1167-1203.

Folk RL & Ward W 1957. Brazos River bar: A study in the significance of grain size parameters. *J. Sed. Petrol*., 27: 3-26.

Friedman GM 1967. Dynamic process and statistical parameters compared for size-frequency distribution of beach and river sands. *J. Sed. Petrol*., 37: 327-354.

Friedman GM 1975. Differences in size distributions of populations of particles among sands of various origins. *Sed*., 26: 3 – 32.

Friedman GM 1979. Dynamic process and statistical parameters compared for size-frequency distribution of beach and river sands. *J. Sed. Petrol*., 37: 327-354.

Friedman GM & Sanders JE 1978. Principles of sedimentology. John Willey and Sons, New York, 792.

Guiraud M 1990. Tectono-sedimentary framework of the Early-Cretaceous continental Bima formation (Upper Benue Trough, NE, Nigeria). *J. Afr. Earth Sci*., 10(1/2): 342–353.

Guiraud R, Binks RM, Fairhead JD & Wilson M 1992. Chronology and geodynamic setting of Cretaceous - Cenozoic rifting in West and Central Africa. In: Ziegler PA (Ed.), Geodynamics of Rifting, Vol. II. Case History Studies on Rifts: North and South America, Africa-Arabia. Tect., 213:227-234.

Hubert JF 1962. A Zircon–Tourmaline–Rutile maturity index and interdependence of the composition of heavy minerals assemblages with the gross composition and texture of sandstone. *J. Sed. Petrol*., 52: 440-450.

Ingersoll RV, Bullard TF, Ford RL, Grimm JP, Pickle JD & Sares SW 1984. The effects of grain size on data modes: a test of the Gazzi-Dickinson point-counting method. *J. Sed. Petrol*., 46: 620–632.

Luttig G 1962. The shape of pebbles in the continental, fluviatile and marine facies. *Int. Ass. Sci. Hydro. Pub.*, 59: 235-258.

Martins LR 1965. Significance of skewness and kurtosis in environmental interpretation. *J. Sed. Petrol*., 35(3): 768-770.

Martins LR, Potter PE, Martins IP & Wolff IM 1997. Grain-size and modern sedimentary environments. Congreso Latinoamericano de Sedimentologia, 1º. *Memorias Tomo* II: 67-71.

Martins LR 2003. Recent sediments and grain-size analysis. *Gravel*, 1: 90-105.

Maurin JC, Benkhelil J & Robineau B 1986. Fault rocks of the Kaltungo lineament (NE-Nigeria) and their relationships with the Benue Trough. *J. Geo. Soc. Lon*., 143: 587-599.

Moulin M, Aslanian D & Unternehr P 2010. A new starting point for the south and equatorial Atlantic Ocean. *Earth Sci. Rev*., 98: 1-37.

Nwajide CS & Hoque M 1982. Pebble morphometry as an aid in environmental diagnosis: an example from the middle Benue Trough, Nigeria. *J. Min. and Geol.*, 19(1): 114-120.

Nwajide CS 2013. Geology of Nigeria's Sedimentary Basins.CSS Bookshop Ltd., Lagos, p. 565.

Ofoegbu CO 1984. A model for the tectonic evolution of the Benue Trough of Nigeria. *Geologische Rundschau*, 73: 1007-1018.

Olade MA 1975. Evolution of Nigeria's Benue Trough (Aulacogen): A tectonic model. *Geol. Mgt*., 112/06: 575-583.

Opeloye SA 2012. Lithofacies association in the Bima Sandstone of the Upper Benue Trough, Nigeria. *The Pac. J. Sci. and Tech*., 13(2): 417-427.

Pettijohn FJ 1984. Sedimentary Rocks. 3rd ed. C.B.S. Publishing Co., Texas, p. 628.

Pettijohn FJ, Potter PE & Siever R 1973. Sand and Sandstone. Springer-Verlang, Berlin, p. 617.

Pettijohn FJ, Potter PE & Siever R 1987. Sand and Sandstone (2nd ed). Springer, New York, p. 553.

Samaila NK, Braide SP, Dike EFC & Suh CE 2005. Study of soft-sediments structures in the Cretaceous Bima Sandstone, Upper Benue Trough, northeastern Nigeria. *J. Min. and Geol*., 41(1): 81-86.

Sames CW 1966. Morphometric data of some recent pebbles associated and application to ancient deposits. *J. Sed. Petrol*., 36: 126-142.

Selley RC 1975. An introduction to Sedimentology. Acad. Press Inc., Lon., 416.

Sneed ED & Folk RL 1958. Pebbles in the Lower Colorado River, Texas: A study in particle morphogenesis. *J. Geol*., 66: 114–150.

Tickell, F.G. (1931): The examination of fragment rocks. Stanford University Press, California. 127.

Tucker ME 1988. Sedimentary Petrology: An Introduction. Blackwell Scientific Publication, London, 252.

Tukur A, Samaila NK, Grimes ST, Kariya II & Chaanda MS 2015. Two member subdivision of the Bima Sandstone, Upper Benue Trough, Nigeria: Based on sedimentological data. *J. Afr. Earth Sci.*, 104: 140–158.

Visher GS 1969. Grain-size distribution and depositional processes. *J. Sed. Petrol*., 39(3): 1074 – 1106.

Weltje GJ & von Eynatten H 2004. Quantitative provenance analysis of sediments: Review and outlook. *Sed. Geol*., 171: 1 – 11.

Wentworth CK 1922. A scale of grade and class terms for clastic sediments. *J. Geol*., 30: 377 – 392.

Whiteman A 1982. Nigeria: Its Petroleum Geology, Resources, and Potentials. Graham and Trotman, London, 394.

Zaborski PM, Ugodulunwa F, Idornigie A, Nnabo P & Ibe K 1997. Stratigraphy and structure of the Cretaceous Gongola basin NE, Nigeria. *Bull. Centres Res. Explore. Prod. Elf Aquitaine*, 21(1): 153–185.

Zaborski PM 2003. Guide to the Cretaceous system in the upper part of the Upper Benue Trough, NE, Nigeria. *Afr. Geosci. Rev*., 10(1 & 2): 13–32.

Zhou T, Wu C, Yuan B, Shi Z, Wang J, Zhu W, Zhou Y, Jiang X, Zhao J, Wang J & Ma J 2019. New insights into multiple provenances evolution of the Jurassic from heavy minerals characteristics in southern Junggar Basin, NW China. *Petroleum Exploration and Development*, 46(1): 67-81.